UNIVERSITI PUTRA MALAYSIA

BIOGLASS-CERAMIC FOR BIOMEDICAL APPLICATIONS: EFFECTS OF VARIED PERCENTAGE OF CALCIUM OXIDE (CaO) DERIVED FROM EGGSHELLS IN CALCIUM FLUOROALUMINOSILICATE (CFAS) BIOGLASS-CERAMIC AT DIFFERENT SINTERING TEMPERATURES

MIMI NUR `ADILAH BINTI SAMAD

BIOGLASS-CERAMIC FOR BIOMEDICAL APPLICATIONS: EFFECTS OF VARIED PERCENTAGE OF CALCIUM OXIDE (CaO) DERIVED FROM EGGSHELLS IN CALCIUM FLUOROALUMINOSILICATE (CFAS) BIOGLASS-CERAMIC AT DIFFERENT SINTERING TEMPERATURES

By

MIMI NUR `ADILAH BINTI SAMAD

Thesis Submitted to the Department of Physics, Universiti Putra Malaysia, in partial Fulfilment of the Requirements for the Degree Bachelor of Science in Materials Science with Honours

February 2022

DEDICATION

I owe my deepest gratitude to my parents, especially my beloved mother, Zaiton binti Abd. Aziz, for her endless prayers, love, sacrifices and support throughout my thesis preparation. For making me what I am today, I can never thank her enough but to dedicate all my hard work throughout my study and life to her. I also express my gratitude to my family, especially my sisters and brother for supporting my study.

Finally, thank you Izyan Fatihah binti Abdul Fatah for being my mentor and best friend since the first day of my degree. I would love to thank my closest friends Siti Sarah binti Mohamad Pauzi, Nur Afiqah binti Badrulhisham, Irdina binti Shahrin, and Nur Illya Aizzah binti Anwar for giving me continuous supports. Also, I truly appreciate all my friends who directly and indirectly contributed to this research work.

ABSTRACT

Bioglass-ceramic for biomedical applications: effects of varied percentage of calcium oxide (CaO) derived from eggshells in calcium fluoroaluminosilicate (CFAS) bioglass-ceramic at different sintering temperatures

by

Mimi Nur `Adilah binti Samad

199195

February 2022

Supervisor: Dr. Nor Kamilah binti Sa'at

Faculty: Faculty of Science

This research aims to study about the effects of varied percentage of calcium oxide (CaO) derived from eggshells in calcium fluoroaluminosilicate (CFAS) bioglass-ceramic at different sintering temperature. The compositions of CaO were varied for four different batches named B1, B2, B3 and B4 with 24 wt.%, 21 wt.%, 18 wt.%, and 15 wt.%, respectively. The varied sintering temperatures for each batch were room temperature, 650 °C, 750 °C, 850 °C, and 950 °C. The CFAS glass ceramic samples were synthesized from waste materials such as eggshells and soda lime silicate (SLS) glass by using melt quenching technique. The produced CFAS glass ceramic samples were analyzed by various characterization methods such as density, molar volume, linear shrinkage, and X-Ray Diffraction (XRD) to interpreted phases of the glass ceramic samples.

ABSTRAK

Bio-kaca seramik untuk aplikasi bioperubatan: kesan peratusan kalsium oksida (CaO) berbeza yang diperolehi daripada kulit telur di dalam kalsium fluoroaluminosilikat (CFAS) bio-kaca seramik pada suhu pensinteran yang berbeza

oleh

Mimi Nur `Adilah binti Samad

199195

Februari 2022

Penyelia: Dr. Nor Kamilah binti Sa'at

Faculti: Fakulti Sains

Penyelidikan ini bertujuan untuk mengkaji tentang kesan peratusan berbeza-beza kalsium oksida (CaO) yang diperoleh daripada kulit telur dalam bioglass-seramik kalsium fluoroaluminosilikat (CFAS) pada suhu pensinteran yang berbeza. Komposisi CaO dipelbagaikan untuk empat kelompok berbeza yang dinamakan B1, B2, B3 dan B4 dengan masing-masing 24 wt.%, 21 wt.%, 18 wt.%, dan 15 wt.%. Suhu pensinteran yang berbeza bagi setiap kelompok ialah suhu bilik, 650 °C, 750 °C, 850 °C dan 950 °C. Sampel seramik kaca CFAS telah disintesis daripada bahan buangan seperti kulit telur dan kaca soda limau silikat (SLS) dengan menggunakan teknik pelindapkejutan cair. Sampel seramik kaca CFAS yang dihasilkan telah dianalisis dengan pelbagai kaedah pencirian seperti ketumpatan, isipadu molar, pengecutan linear, dan Pembelauan X-Ray (XRD) untuk mentafsir fasa sampel seramik kaca.

ACKNOWLEDGEMENT

First and foremost, praise and thanks to God, the Almighty, for His showers of blessings throughout my research work to successfully complete the research. The success and outcome of this project required a lot of guidance and assistance from many people. I am incredibly privileged to get this all along with completing my research work and thesis preparation. I have done all that is only due to such supervision and assistance, and I would not forget to thank them.

I respect and thank my supervisor Dr. Nor Kamilah binti Sa'at, for all support and guidance, which made me complete the project duly. I am incredibly thankful to her for providing invaluable guidance and willingness to provide feedback throughout this research, although he had a busy schedule throughout these two semesters.

I heartily thank my postgraduate senior Nur Quratul Aini binti Ismail for her encouragement, timely support, and guidance until completing my project work by providing all the necessary information.

I am thankful to all technicians and staffs at the Physics Department UPM, for their guidance, which helped me complete my project work.

TABLE OF CONTENT

LIST OF FIGURES

LIST OF TABLES

LIST OF ABBREVIATIONS

CFAS	Calcium Fluoroaluminosilicate
ES	Eggshells
SLS	Soda Lime Silicate
wt%	Weight percent
SDG	Sustainable Development Goals
HCA	Biologically Active Hydroxyapatite
SBF	Simulated Body Fluid
GC	Glass-ceramic
BGC	Bioglass-ceramic
XRD	X-Ray Diffraction
TGA	Thermogravimetric Analysis
DSC	Differential Scanning Calorimetry
BO	Bridging Oxygens
Tg	Glass Transition
DTA	Differential Thermal Analysis
rpm	Revolutions Per Minute
XRF	X-ray Fluorescence
CTE	Coefficient of Thermal Expansion
FTIR	Fourier Transform Infrared Spectroscopy
FESEM	Field Emission Scanning Electron Microscopy
µ	$1x10^{-6}$

CHAPTER 1

INTRODUCTION

1.0 Background of Research

For thousands of years, glasses have been used by humankind in many applications and forms. Glasses are useful from simple and common materials such as bottles, containers, light bulbs, windows to technical applications such as computer screens, television tubes, spectacles, laboratory wear, and optical fibres or even for artistic purposes (Gutzow et al, 2012) (Doremus, 1994) (Paul, 1990). Glasses are different from crystalline solids as they do not have long-range order and significant symmetrical atomic arrangements (Ferreira, 2018). Despite of that, glass constituent atoms are well-organized in a short-range which depends on the glass composition itself (Shelby, 2005) (Vallet-Regi, 2014). Glass structure is unstable due to the relaxation towards the state of supercooled liquid and this supercooled liquid is metastable with respect to equilibrium crystal (Ferreira, 2018) (Mauro et al., 2008). The structure of the glasses has given many effects on their properties such as density, stability, ion release in aqueous environments, solubility, and coefficient of thermal expansion (CTE) (Ferreira, 2018).

By using two principal methods, glasses can be produced by melt-quenching method and sol-gel processes. Glasses have excellent advantages compare to crystalline substances as they can be synthesized into a virtually unlimited compositions range while crystalline phases possess a well-defined and a constant stoichiometry (Vallet-Regi, 2014). The other properties of glass are it can be changed and adjusted by doping. As an example, a small number of other oxides is added to the composition of the glass. This will allow the controlled release of ionic species (Ferreira, 2018). This feature is extremely important in

bioactive glass to provide them with potential therapeutic actions while releasing ions that will stimulate osteoinduction or also known as cells differentiation and can act as antimicrobial agents (Jones et al., 2012).

For more than four decades, bioactive glasses have been widely studied for medical applications (Ferreira, 2018). Throughout the evolution, bioactive-glasses can be distinguished into several families. In 1969, Hench discovered the first melt-derived bioactive glass, which is Bioglass 45S5 (Montazerian et al., 2016). Next, in 1991, Hench proposed the bioactive gel-derived glasses (Kokubo, 2008). Currently, Vallet-Regi et al designed the bioactive glasses with ordered mesoporosity (Salinas et al., 2013).

The properties that can be shown by the bioactive glasses are osteoconduction and osteoinduction. These both properties can be used in vast applications such as scaffolding, drug delivery, soft tissue engineering, coatings, and bone grafting. Although bioglass-ceramics have excellent bioactive properties, they have low mechanical strength and low fracture toughness, K_{IC}. The bending strength that bioglass-ceramics have is approximately 70 MPa and 0.5 $MPa \cdot m^{1/2}$ $K_{IC.}$ These advantages restrict their use that do demand significant loads (Ferreira, 2018). Therefore, to improve the mechanical strength, bioactive glass ceramics have been developed by using various types of glasses in different crystalline precipitation phases under a heat treatment process (Ferreira, 2018). The well-known bioactive glass ceramics available in the market are Cerabone®, Biosilicate®, Ceravital®, and Bioverit® (Kokubo, 2018) (Salinas et al., 2013) (Baino et al., 2016) (Miguez-Pacheco et al., 2015) (Hench, 2013) (Kokubo, 1991).

Glass-ceramics can be defined as polycrystalline materials that contain one or more crystal phases that were embedded into a residual glass and produced by the controlled heat treatment of certain glasses (Ferreira, 2018). Heat treatment can be done in two stages, relatively low temperatures compare to glass transition to induce the internal nucleation

and followed by higher temperature to promote the different growth phases. The crystallinity varies between 0.5% and 99.5%, most frequently between 30% and 70% (Ferreira, 2018). The controlled crystallization proved the materials with amount of properties combinations such as electrical, thermal, biological, and mechanical (Zanotto, 2010) (Montazerian et al., 2015) (Holand, 2012). Bioactive-glass can elicit biological reaction at the interface of the material by the stimulation of cell proliferation, gene response and the bond formation between the materials and the living tissues. The surface of the bioactive-glass ceramics develops a biologically active hydroxyapatite (HCA) layers that interconnect with the bone. HCA layers on the bioactive-glass ceramics are structurally and chemically equivalent to the bone mineral phase (Ferreira, 2018). After the immersion of simulated body fluid (SBF), bonelike HCA is developed on the surface of the sample (Solé et al., 2016).

In term of properties, glass-ceramic (GC) combine the properties of glasses with conventional sintered ceramics benefits. Usually, GCs are manufactured in a process where a pre-manufactured glass is subjected to a particular heat treatment. Then, the glass will partially crystallize, and the GC will develop a structure compromising a glassy (amorphous) phase and at least one phase of embedded crystalline (Höland et al., 2012). There are two categories of GC which are oxide and non-oxide. Oxide GC include borate (B_2O_3), silicate (SiO_2) and germinate (GeO_2) and phosphate (P_2O_5) material type. Non-oxide GC include chalcogenide, metallic and halide type (Solé et al., 2016). GCs can be used in many applications such as cooktops, household appliances, smartphone screens, infrared heating elements, biomedical engineering, household appliances and so much more.

The main difference between bioglass-cramics (BGCs) and and glass-ceramics (GCs) is their compatibility with living cells. Bioactive materials such as BGCs can evoke a specific biological response at the apatite layer while non-bioactive materials such as glass ceramics cannot. One of the most common types of BGCs used in medical sector is calcium fluoroaluminosilicate (CFAS) glass which contain phosphorus and sodium (Ions et al., 2017). CFAS glass is potential bioglass that can be used in biomedical application. CFAS glass consists of an inorganic polymeric network embedded in a silicon and an aluminium matrix. BGCs are used in medical sector as artificial vertebrae, iliac bones, orthopaedic, dentistry and more (Khiri etal., 2020).

In this study, CFAS glass was synthesized by using commercial and waste materials. The waste materials were eggshells (ES) and soda lime silicate (SLS) glass that can be obtained from the glass bottle. The major chemical compositions of SLS glass are SiO_2 (73.9 wt. %) and CaO (11.2 wt. %) (Khiri et al., 2020). SLS and ES are waste products that will be based of silica and calcium oxide, respectively. The mineralized shell composition of the egg is approximately 96% calcium carbonate. The calcium carbonate will undergo calcination process to obtain calcium oxide (Hinchke et al., 2012). The aluminium oxide, calcium fluoride, and phosphorus pentoxide were the commercial products (Khiri et al., 2020).

1.2 Problem Statements

CFAS can be produced by combination commercial and waste materials. Silicon dioxide and calcium oxide can be obtained from eggshell and SLS glass as waste products meanwhile aluminium oxide, calcium fluoride, and phosphorus pentoxide were the commercial products (Khiri et al., 2020). By using waste materials, we can reduce the domestic waste efficiently. Besides that, we can reduce the CFAS production cost thus this GC can be more affordable for the people to obtain medical services in future. This is a good initiative to help Malaysia in achieving the Sustainable Development Goals (SDG). The SDG are world's shared plan to end the extreme poverty, protect the planet and reduce inequality by 2030. CFAS is synthesized by using melt-quench method. CFAS is chosen in this research because of its excellent biomedical properties. More research is required to improve these potential materials for a better future in medical sector.

1.3 Objectives

The objectives of this research are to synthesise the CFAS bioglass-ceramic at different percentage of calcium oxide by using melt-quenching method and to investigate structural, of the calcium CFAS bioglass-ceramic with different content percentage of calcium oxide atdifferent sintering temperature.

1.4 Thesis Overview

This thesis comprehends five chapters that describe the theories, methods, and results of the experimental research performed. The first chapter is an introduction to the field of a research study. In this chapter, a few points are highlighted: problem statement of the study, objectives of the research, and the thesis overview stated to elucidate the research. Chapter two delineates the literature review that enumerates and describes the basis of the research study, along with the characteristics of the main constituents of the study. The process and characterization methods have also been clarified in this chapter. Chapter three narrates the methodology or the procedure for the research work. All the research flows, raw materials, the machines used, and experimental analysis were also explained in-depth without summarizing. In chapter four, results and discussions from the experiment conducted, including the samples' structure properties effects, were presented. Finally, yet importantly, the summary and recommendation for future research work are specified in chapter five.

CHAPTER 2

LITERATURE REVIEW

2.1 Calcium Fluoroaluminosilicate (CFAS) Bioglass-Ceramics

CFAS is one of silicate based bioglass-ceramics system, Na_2O-CaO-P_2O_5-SiO_2. Other than that there are Na_2O-Al_2O_3-B_2O_3-SiO_2 and Li_2O-Al_2O_3-SiO_2 (Brinker et al., 1990) (Hench et al., 1990) (Klein, 1990). These silicate glass ceramics have large surface area, high porosity and purity index within the BG contribute to high level of reactivity as biomaterial. CFAS is one out of several formulas of silicate based bioglass-ceramics. CFAS glasses are the basis of degradable glasses and mould flux glasses (Khiri et al., 2020).

The CFAS can be produced by using five main compounds which are eggshells (ES), soda lime silicate (SLS) glass, Al_2O_3, CaF_2 and P_2O_5 based on a chemical composition of $15CaO$-$40SiO_2$-$5CaF_2$-$20P_2O_5$-$20Al_2O_3$ which were 20% phosphorus pentoxide as dehydrating agent, 40% silica as primary component of the glass, 5% calcium fluoride as dehydration catalyst, 15% calcium oxide renders the glass insoluble, and 20% alumina to improve the properties and depress the glass devitrification (Khiri et al., 2020) (Moulton et al., 2021) (Chareev, 2019) (Pentoxide, 2002) (Nezafati et al., 2011) (Liu et al., n.d.). Silicon dioxide was obtained from soda lime silica (SLS) glass bottles waste for raw waste materials of the glass synthesis (Khiri et al., 2020). Meanwhile, calcium oxide (CaO) is obtained from waste product, eggshells (Khiri et al., 2020). Eggshells primarily contain calcium carbonate ($CaCO_3$) but then undergo through a calcination process to release the carbon dioxide in the calcium carbonate ($CaCO_3$) (Hinchke et al., 2012).

In the CFAS glass ceramic, fluorine is a GC integral component. Besides that, it is also known as a powerful network disrupter. Fluorine disrupts the glass networks, replacing the bridging oxygens, BO, by non-bridging fluorine. Other than that, fluorine is thought to reduce the temperature of glass transition (T_g), enhance crystallization, reduce refractive index, reduce viscosity, and increase glass degradability (Stamboulis et al., 2004).

Silicon (Si) is an important basic element in human body which is essential for the development of bone. Silicon in the silicate based bioglass-ceramics such as CFAS plays important role in collagen biosynthesis, have beneficial effect on proteins phosphorylation, nucleotides, and saccharides. This element is also important for the cytoskeletons formation and other mechanical cellular structures or supportive function. CFAS is a silicate based bioglass-ceramic materials which have shown excellent potential in bone-related in tissue regeneration and tissue engineering applications (Zhou et al., 2015). With proper composition, silicate-based bioactive materials are promising the regeneration materials of bone.

GC materials have interesting mechanical and biological properties. Bioactive glasses have osteoinduction and osteoconduction properties (Montazerian et al., 2016). Bioactive glass responds with biological cells at the interface of the material. It stimulates bond formation between biology tissues and the material which is known as cell proliferation. Common characteristics of bioactive GCs is they have a special layer known as hydroxycarbonate apatite (HCA) layer that bonds to bone (Montazerian et al., 2016). CFAS glass is a fluoride-containing bioglass-ceramics that contain fluoroapatite. This material increases the density of GC (Brauer et al., 2012). The developments by numerous of research provide hints to achieve many advances in practical applications requirement in future.

2.2 Melt-quenching Method Technique and Sol-gel Method

Both sol-gel and melt-quenching method technique is used to produce bioactive glass (Ions et al., 2017). Melt quenching is a traditional technique of glass making and includes the ingredients mixing, heating at specific temperature, and quenching the glass melt to get a glass frit. The sol-gel technique is another alternative low temperature chemical approach to produce the bioactive glass (Khurshid et al., 2019). These both techniques affect the results of the glass-ceramics.

2.2.1 Melt-quenching Method Technique

Melt-quenching method bioactive glass synthetization are simple and available in commercial (Methods, 2020). The disadvantages of this method are the bioactive glass have low homogeneity and low bioactivity due to its low surface area to react with living cells (Salinas, 2014). In this method, SLS glass bottle and eggshells are prepared as resources of SiO_2 and CaO in the bioactive glass compositions (Khiri et al., 2020). Melt-quenching method has several important steps which are mixing, homogenizing, calcining and fusing glass precursors which is simplified in Figure 2.1 (Methods, 2020) (Srinivasan et al., 2015) (Khiri et al., 2020) (Methods, 2020) (Srinivasan et al., 2015). After heated the precursor mixtures, the melt will bequenched in cold water or cast in graphite molds (Methods, 2020).

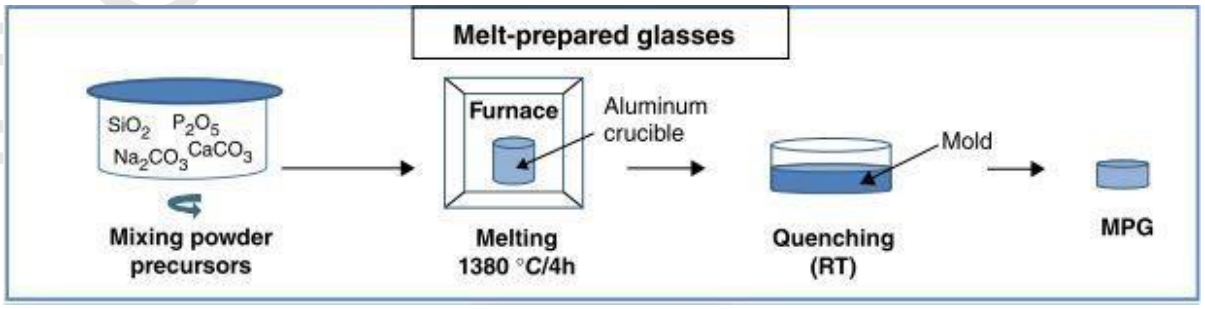

Figure 2.1: The simplified process of producing glass by using melt-quenching method example

2.2.2 Sol-gel Method

CFAS glass can also be synthesized by using sol-gel method as other alternative but there are some pros and cons in this method (Srinivasan et al., 2015). Sol-gel synthesized bioactive glasses have more advantages compare to glass that is melt produced in aspect of better bioactivity and porosity. Besides that, the other advantages of sol-gel technique are such as low-temperature processing, high purity and homogeneity, more composition freedom, microstructural features tenability and has higher bioactivity and degradation (Khurshid et al., 2019).

The disadvantages of using sol-gel method to synthesize bioactive glass are expensive raw ingredients, the production process is long, and complex compared to the melt-produced bioactive glass. This method has limit for some biomedical applications as the sol-gel derived bioactive glass has high rate of degradation (Khurshid et al., 2020). Seven basics steps in sol-gel technique are mixing the precursors, casting, aging, gelation (Linden et al., 2021), controlled drying, dehydration or stabilization and densification (Valverde, 2019). First, the precursors are mixed on a substrate to form film or powders that will end up dispersed uniformly.

Next, the product undergoes casting process then followed by aging and gelation for several days until it is ready to dry in the oven. Lastly, firing process such as controlled drying, dehydration and densification are done to increase polycondensation, improve mechanical properties and structural stability (Brinker et al., 1990) (Hench, 1990) (Salinas, 2014). Based on Figure 2.2, the sol-gel process is simplified (Salinas, 2014).

Sol-gel process is a process of forming oxide network through polycondensation reactions of molecular precursor in a liquid. In general, this process starts with a silicate solution and then forming a sol. Then it is transformed into a gel and lastly a dry gel will be obtained. The formed dry gel formed by a three-dimensional silica with various sizes of numerous pores interconnected (Pirayesh et al., 2013).

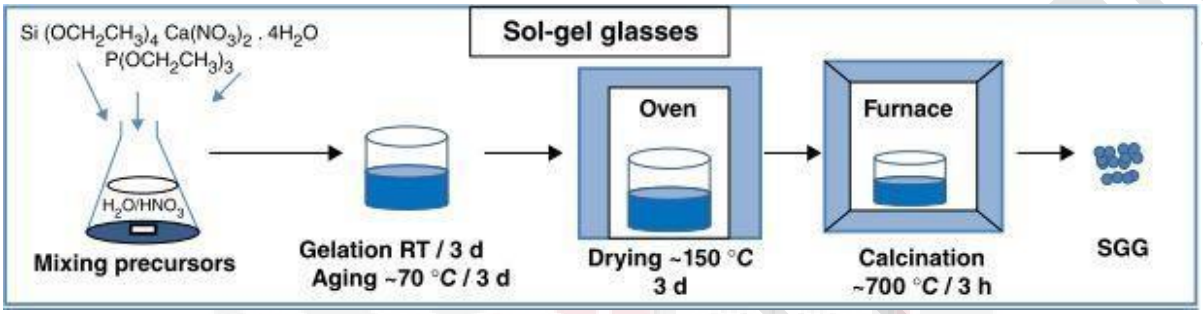

Figure 2.2: The simplified process of producing glass by using sol-gel method

2.3 Waste Source for CFAS

In this study, CFAS glass was synthesized by using commercial and waste materials which were eggshells (ES) and soda lime silicate (SLS) glass that can be obtained from the glass bottle. The mineralized shell composition of the egg is approximately 96% calcium carbonate. The calcium carbonate will undergo calcination process to obtain calcium oxide (Hinchke et al., 2012).

2.3.1 Silicon dioxide (SiO_2)

Silicon dioxide is one of the important components in CFAS glass ceramic materials. There are several alternative sources to obtain this compound such as extracting it from domestic wastes which are rice straw and soda lime silicate (SLS) glass. To extract the SiO_2 from rice straw, the process starts from drying the rice straw by putting it under the sunlight. After it is dried, the weighed rice straw is burned open without using fuel. Then, it is weighed and put into a porcelain dish and heated in the furnace at temperature of 400 °C for two hours and increased to 900 °C for an hour. Subsequently, it is washed with 3% HCl to reduce the impurities in the sample. Lastly the rice straw is heated on the hot plate and stirred thoroughly by using a magnetic stirrer. The final product is filtered and heated at temperature of 900 °C for an hour (Nazopatul et al., 2018).

Besides, SiO_2 can alternatively obtained from waste material, soda lime silicate glass bottle that can easily be found in houses and grocery stores. Firstly, to remove the impurities, the SLS glass is washed with water. Then, it is dried under the sunlight and crushed into smaller pieces by using hammer. The small frits of the glass are then crush by using steel plunger to get the fine powder. After that, the powder is ground by using pestle and mortar to obtain the finer powder and lastly sieved using the 45 μm sieve (Khiri et al., 2020).

2.3.2 Calcium Oxide (CaO)

CaO can be extracted from organic materials such as eggshells (ES) and clam shells (CS). To extract this compound from CS, it is collected and cleaned to remove the impurities, then dried. The CS undergo the calcination process in the furnace at 900 °C for two hours, then sieved into the 45 µm sieve (Khiri et al., 2020).

Alternatively, CaO can also be extracted from ES which are easily can be found in the eating stalls. First, the ES are collected and washed with water to remove impurities. After that, dry the ES under sunlight for several hours until it is dried. Next, crush ES into small pieces and put into the furnace at atmospheric oxygen condition at 900 °C for two hours to undergo calcination process. The powder is sieved through the 45 µm sieve (Tangboriboon et al., 2012) (Mohadi, 2016) (Hincke et al., 2012)

2.4 Effects of Different CaO Percentage on Glass-Ceramics System

CaO was studied for its influence on the microstructure, densification, thermal, dielectric, and mechanical properties of $Li_2O–Al_2O_3–SiO_2$ (LAS) glass–ceramics. CaO stimulates the production of the $CaMgSi_2O_6$ phase, which may increase microstructure, densification, and mechanical properties. With the addition of CaO, the glass–coefficient ceramics of thermal expansion rises and approaches that of silicon chips (Qing et al., 2016).

2.4.1 Mechanical Properties

Figure 2.3 depicts the effects of the CaO and SiO_2 ratios on the three-point bending strength and CTE of LAS glass–ceramics sintered at 800 °C for 0.5 hours. On the one hand, glass–ceramic has a bending strength of 90 MPa, which increases to 154 MPa when 2.1 wt. % CaO is added. This suggests that adding CaO has a considerable impact on mechanical properties. As the amount of CaO in the solution increases, the bending strength decreases. On the other side, when the CaO concentration in LAS glass–ceramic rises, the CTE value climbs linearly from 1.2 to 2.99×10^{-6} /°C. The CTE of a glass–ceramic is often determined by the CTE values of its crystalline and glassy phases. The rise in CTE is attributed to an increase in the glass-ceramic phase, which has a high CTE value of 8.59×10^{-6} /°C, according to XRD research (Kim et al., 2012). To avoid thermal stresses produced by thermal expansion mismatch between silicon chips and the substrate, the CTE must be as close to that of silicon as possible (3.59×10^{-6} /°C). The CTE of a material doped with 6.1 wt. % CaO is 2.999×10^{-6} /°C. which is extremely similar to silicon (Chen et al., 2004).

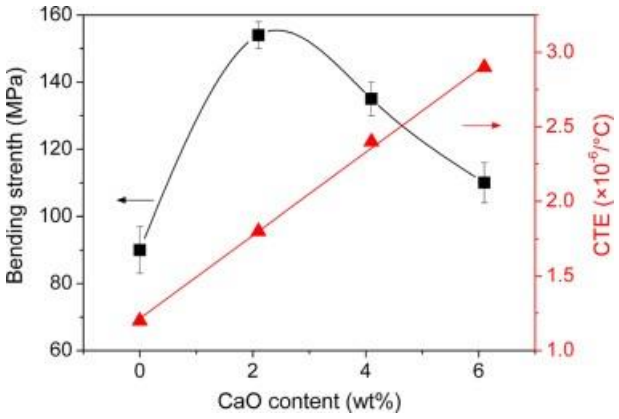

Figure 2.3: The CTE and bending strength of LAS glass–ceramics fired at 800 °C for 0.5 hour

2.4.2 Density

The bulk densities of glass–ceramics decrease noticeably with increasing CaO concentration, as seen in Figure 2.4. Furthermore, the bulk densities of all GC samples in this study drop as the sintering temperature rises. This glass–ceramic has a low softening temperature, which can enhance the development of liquid phase at low sintering temperatures, as indicated in differential thermal analysis (DTA) curves. The liquid phase aids the densification of LAS glass–ceramics by speeding up mass movement. Furthermore, when the sintering temperature rises, the bulk densities of all samples decrease, which is likely due to inhomogeneous evaporation of the liquid phase during the sintering process.

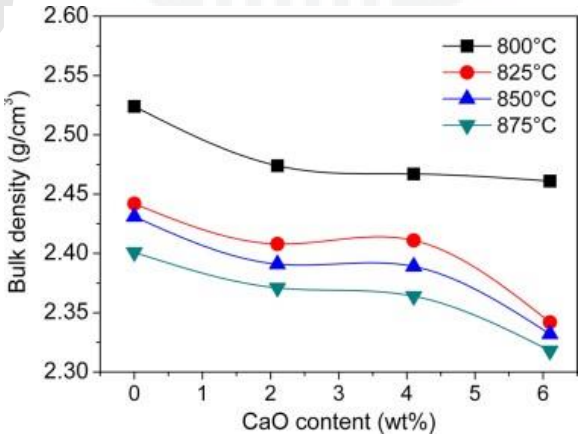

Figure 2.4: bulk densities for four different samples at different temperatures

2.4.3 Linear Shrinkage

Figure 2.5 (a) and (b) show the percent of linear shrinkage of the four LAS samples sintered at 800 °C for 0.5 hour and the fluctuation of the percent of linear shrinkage of the sample LAS2 with sintering temperature. The percentage of linear shrinkage rises with increasing CaO concentration, as seen in Figure 2.5 (b). Furthermore, as demonstrated in Figure 2.5, the percent of linear shrinkage reduces linearly as the sintering temperature rises (a). The liquid glass might penetrate the ceramic-rich areas and fill the capillary pore channels between the filler grains during the sintering process (Kim et al., 2012). As a result, the liquid glass is critical for the densification sintering process. As a result, fluctuations in LAS glass–ceramic shrinkage should be related to changes in the liquid glass.

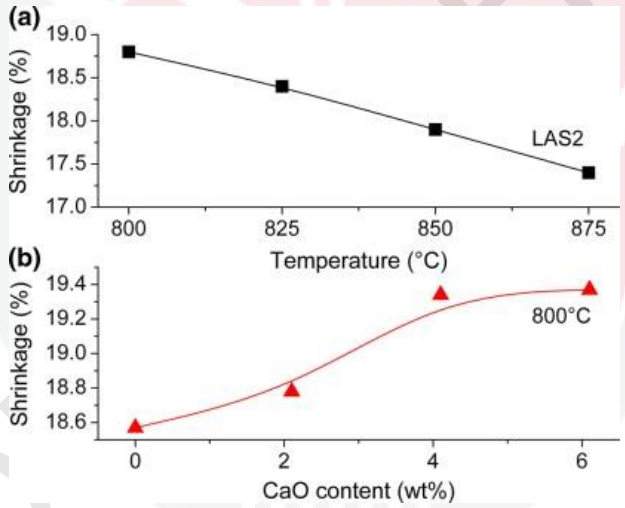

Figure 2.5 The shrinkage percentage of sample LAS2 with (a) varied sintering temperature and (b) CaO compositions

2.4.4 Structure

Figure 2.6 depicts SEM micrographs of the cross-sections of four LAS samples heat-treated at 800 °C for 0.5 hour. It is obvious that the sample LAS1 (without CaO addition) has a large number of holes, indicating that it has a loose microstructure. However, the inclusion of CaO reduces the number of holes in LAS samples, resulting in a thick microstructure. The best microstructure is seen in sample LAS2, which has a CaO concentration of 2.1 wt.%.

However, when the CaO level increases, the microstructure of the LAS glass–ceramic begins to degrade. These findings reveal that adding CaO to the LAS system has a noticeable influence not only on the crystalline phase, but also on the morphology of the glass–ceramics. Archimedes densities of sintered samples were measured and evaluated to determine the effect of CaO concentration and sintering temperature on the densification behavior of LAS glass–ceramics.

The outcomes are shown in Figure 2.4. The results reveal that the bulk densities of LAS glass–ceramics decrease noticeably as the CaO component increases. It might be attributed mostly to a rise in the $CaMgSi_2O_6$ phase, which has a lower bulk density of 328 g/cm^3 than other crystalline phases. Furthermore, the bulk densities of all LAS samples fall as the sintering temperature rises.

As illustrated in the DTA curves, this LAS glass–ceramic has a low softening temperature, which can facilitate liquid phase formation at low sintering temperatures. Because the liquid phase promotes mass transfer, it aids in the densification of LAS glass–ceramics. Furthermore, the bulk densities of all samples decrease as the sintering temperature rises, which is most likely due to inhomogeneous evaporation of the liquid phase during the sintering process.

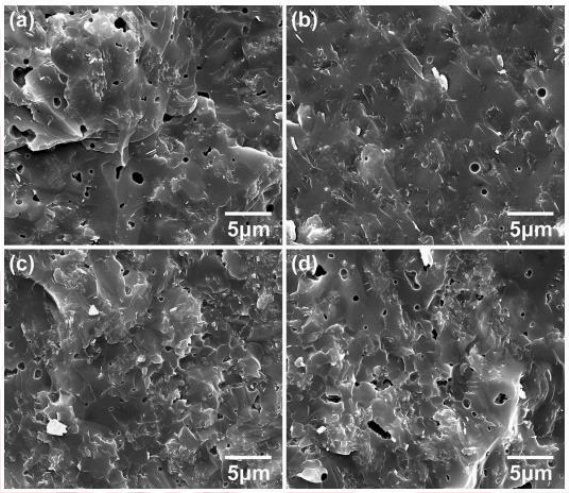

Figure 2.6: SEM micrographs of LAS sample

CHAPTER 3

METHODOLOGY

3.1 Weight Composition of CFAS Glass-Ceramic

There are five samples of CFAS glass with varied wt. % of CaO and CaF_2 as listed in the Table 3.1**.** The composition of CFAS glass is consisted of 44 wt. % SiO_2 + (24 – x) wt. % CaO + 20 wt.% Na_2O + 6wt.% Al_2O_3 + 6wt.% P_2O_5 + x wt.% CaF_2 where x values are 0,3,6, and 9. The mass of each batch is 40 g. Table 3.1 is the actual mass calculated from the weight percent in grams.

Table 3.1: Wt.% of CaO and CaF_2 in each batch

sample name	wt.%	
	CaO	CaF_2
B1	24	0
B2	21	3
B3	18	6
B4	15	9

Table 3.2: Actual mass of each composition in each batch

sample name	mass (g)					
	SiO_2	CaO	Na_2O	Al_2O_3	P_2O_5	CaF_2
B1	17.6	9.6	8.0	2.4	2.4	0
B2	17.6	8.4	8.0	2.4	2.4	1.2
B3	17.6	7.2	8.0	2.4	2.4	2.4
B4	17.6	6.0	8.0	2.4	2.4	3.6

By using five chemical compound which are eggshells, SLS glass, CaF_2, Al_2O_3 and P_2O_5, the CFAS glass was produced. SLS glass and eggshells were waste products from local food stalls that will be source of silica (SiO_2) and calcium oxide (CaO_2) respectively. The aluminium oxide (Al_2O_3) from Alfa Aesar (a Johnson Matthey company), calcium fluoride (CaF_2) from R&M Chemicals, and phosphorus pentoxide (P_2O_5) also from Alfa Aesar (a Johnson Matthey company), were the commercial products. Both calcium oxide (CaO) and silica (SiO_2) are obtained from eggshells and SLS glass. Eggshells contain about 96% calcium carbonate and can be extracted to obtain calcium oxide by a process known as calcination process. Figure 3.1 is how the calcination process was done.

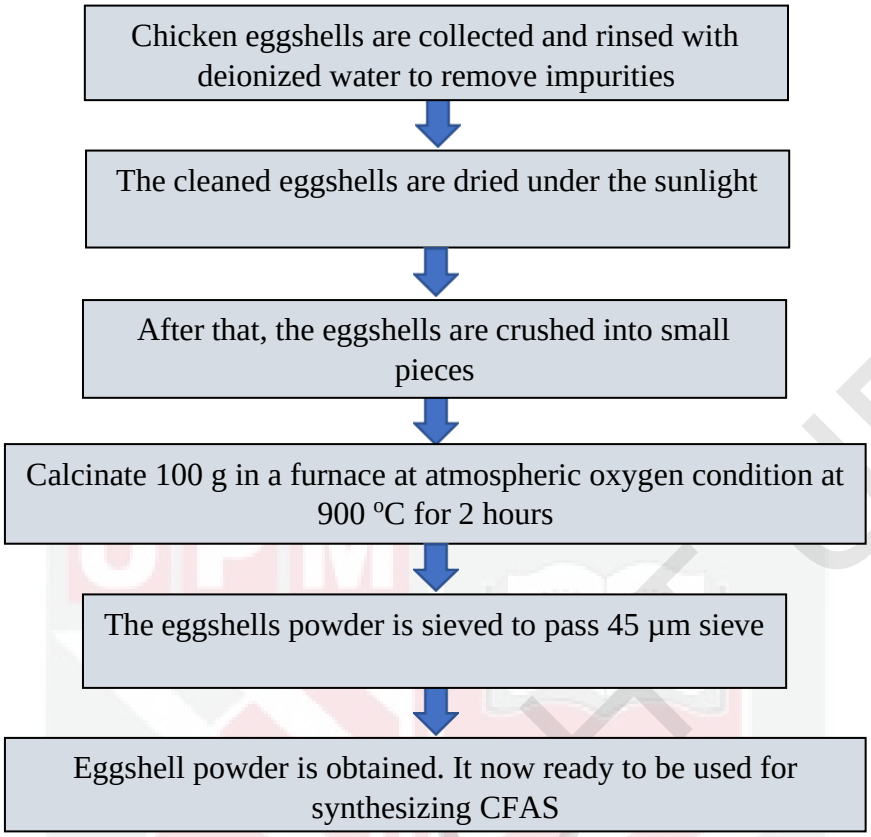

Figure 3.1: Calcination process

Different weight of each chemical compound of CFAS glass composition that were weighed previously by using electronic digital weighing machine are mixed thoroughly. After the mixing process, the mixture was transferred into milling jar using US Stoneware Jar Mill NA model with approximately 70 rpm, speed range and milled about 30 minutes to obtain a homogeneous mixed powder.

3.2 Melting and Water Quenching

Homogenous powder mixture then is filled in the alumina crucible. It is melted in the LT Furnace model with temperature increment by 10 °C per minute about 4 hours at 1400 °C. The melting temperature of the silica based bioglass-ceramic is between 1350 °C to 1400 °C in Pt-Rh crucible or 1350 °C to 1500 °C in platinum crucible. In this research, the melting temperature for CFAS glass ceramic samples is determined by its glass composition (El-Ghannam et al., 2011) (Elsevier, 1982) (Hoppe et al., 2014). The furnace in this research applies the single stage heating process which started from 30 °C and increased to 1400 °C for two hours then the sample is constantly heated at holding temperature for four hours. 15 minutes after holding temperature is added to provide time for quenching process. After that, the melted GC in the alumina crucible is put out and poured into the metal sieve soaked in a pile of tap water quickly. The molten will go through water quenching process where and thermal shock is occurred and produces glass frits. Lastly, place the emptied crucible back into the furnace. The heater button is turned off and the single heating process is let continued for two more hours.

3.3 Crushing, Grinding, and Sieving

Next, the glass frits were crushed and grinded to obtain the powder form by using plunger and hammer. The powder form was sieved using sieve with size of 45 μm in producing a fine powdery form.

3.4 Characterization of CFAS glass

The samples were characterized in physical and structural using various measurements. The measurements were X-Ray Fluorescence (XRF), X-Ray Diffraction (XRD), density, molar volume, and linear shrinkage percentage.

3.4.1 X-Ray Fluorescence (XRF)

XRF is used to determine the elemental composition of material (Simon, 2020). XRF measurement was done on the samples by using an Energy Dispersive X-ray Spectrometer (model EDX-720 Shimadzu). The sample in this CFAS synthetization is in powder form that was sieved at 45 µm in size. Figure 3.2 shows the mechanism of X-Ray radiation from a sample in XRF system. Firstly, the sample is irradiated with high energy x-ray beam emitted from a controlled x-ray tube. Then, the x-ray beam with sufficient energy struck an atom in the sample causing an electron from one of the atom's inner orbital shells dislodged. After that, the atom regains its stability by filling the vacancy left by the dislodged electron just now with another electron from the atom's higher energy orbital shells. Lastly, the electron drops to the lower energy state by releasing a fluorescent x-ray. This energy is equal to the specific difference energy between two quantum states of the electron. XRF analysis basis is this energy measurement (Staff, 2020).

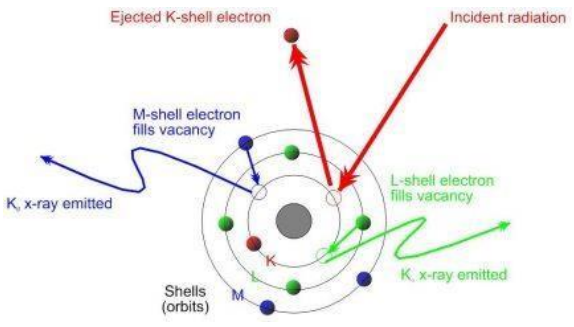

Figure 3.2: The mechanism of X-Ray radiation from a sample in XRF system

3.4.2 X-Ray Diffraction (XRD)

X-ray Diffraction (XRD) machine is used to determine the crystal structure of the CFAS (Paar, 2021), (Albadr et al., 2015), (Pirayesh et al., 2013). The diffraction occurs from plane set as angle 2θ is the diffraction angle with respect to incident radiation. The distribution of electron in the unit cell of the sample will determine the intensities of diffraction. The illustration is shown in Figure 3.3 (Paar, 2021). For this research, the XRD measurement was carried out from angle 20◦ to 80◦. X-ray Phillips (Model PW 1830) with CuKα radiation= 1.5418 Å at 40 kV and 30 mA of the input current was used to identify the structure of the sample. The results obtained then extracted by using X'Pert Highscore software (Khiri et al., 2020). Figure 3.3 shows the result example of XRD measurement analysis of CaO sample (Imtiyaz et al., 2013).

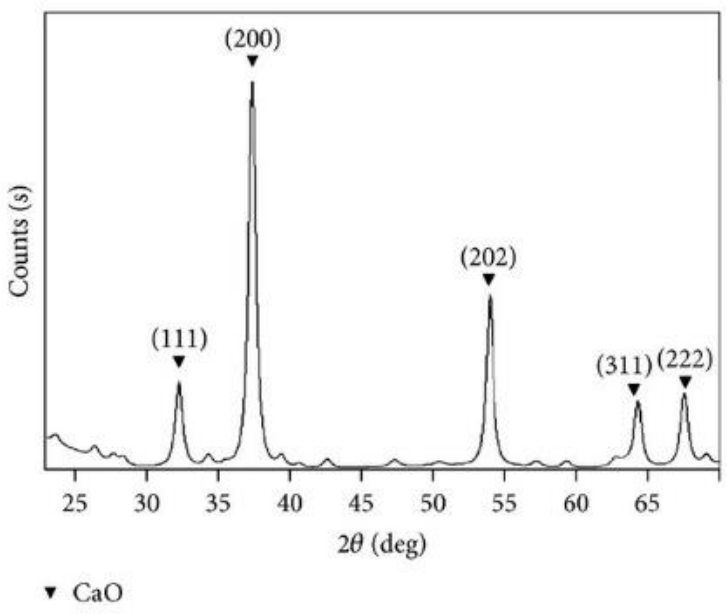

Figure 3.3: The result example of XRD measurement analysis

3.4.3 Density

The density is measured by using Archimedes principle (Brauer et al., 2012). The purpose of doing this measurement is to determine the density of the BGCs. Archimedes' principle states that the buoyant force on an object is equal to the weight of the fluid it displaces (Ridgely, 2010). Specific gravity is the density of an object to a fluid ratio. By using the electronic balance with the accuracy of ± 0.001 g the CFAS in pellet form was weighted in air and water, W_{water} and W_{air}. The density of different ageing time GIC was calculated by using formula Eq. (1):

$$\rho = \frac{W_{air}}{W_{water}} \times \rho \qquad (1)$$

where W_{air} is the weight of sample in air, W_{water} is the weight of sample in distilled water. ρ_w is the density of distilled water. The water density is 1.00 g/cm ^{1}.

3.4.4 Molar Volume

The CFAS molar volume at different wt % were calculated by using Eq. (2):

$$V_m = \frac{M_T}{\rho} \times \rho_w \qquad (2)$$

where M_T is the total of CFAS sample molecular weight, ρ represents the density of the CFAS pellet and ρ_w is the distilled water density (Khiri et al., 2020).

3.4.5 Linear Shrinkage

Linear shrinkage can be measured by using the formula:

$$linear\ shrinkage = \frac{size\ before\ sinter - size\ after\ sinter}{size\ before\ sinter} \times 100\% \quad (3)$$

The measurement tool used is outside micrometer.

CHAPTER 4

RESULTS AND DISCUSSIONS

4.1 Introduction

This chapter discussed the results obtained from various analyses and characterizations that have been carried out within the period of research study. However due to the time constraint, the result of this study only reaches up to density, molar volume, linear shrink and XRF measurements. The result and discussion on other analysis such as phase and structure of the studied sample from XRD and SEM are included by taking from related previous papers to complete and give an idea on the structure of CFAS glass ceramic with varied CaO at different sintering temperature.

4.2 XRF

Table 4.1: Quantitative result for eggshells

ANALYTE	RESULT
CaO	99.480%
K_2O	0.258%
Sc_2O_3	0.107%
Er_2O_3	0.068%
SrO	0.061%
CuO	0.022%
ZrO_2	0.004%

Table 4.1 shows the XRF analysis of eggshells. Based on the obtained results, eggshells contain several analytes such as CaO, K_2O, Sc_2O_3, Er_2O_3, Er_2O_3, SrO, CuO, and ZrO_2. The eggshells contain 99.480% of CaO which is the largest element percentage composition, then followed by 0.258% of K_2O, 0.107% of Sc_2O_3, 0.068% of Er_2O_3, 0.061% of SrO, 0.022% of CuO, and 0.004% of ZrO_2. Other elements have significantly small percentage compositions compare to CaO which only 0.52%. Therefore, the thermal treatment has successfully transformed the chemical composition from calcium carbonate ($CaCO_3$) to calcium oxide (CaO) almost perfectly (Tangboriboon, N et al., 2012).

Table 4.2: Quantitative result for soda lime silicate (SLS) glass

ANALYTE	**RESULT**
SiO_2	59.504%
CaO	36.644%
Fe_2O_3	1.031%
SO_3	0.771%
Sc_2O_3	0.490%
ZnO	0.359%
K_2O	0.330%
Co_2O_3	0.291%
ZrO_2	0.281%
Cr_2O_3	0.110%
SrO	0.063%
CuO	0.49%
Ac	0.039%
NiO	0.038%

Table 4.2 shows the XRF quantitative result for soda lime silicate (SLS) glass. SLS glass contains 59.504% of SiO_2 as its main composition. It also contains 36.644% of CaO and some other elements which are in significantly small percentages respectively (63.356%).

4.3 Density

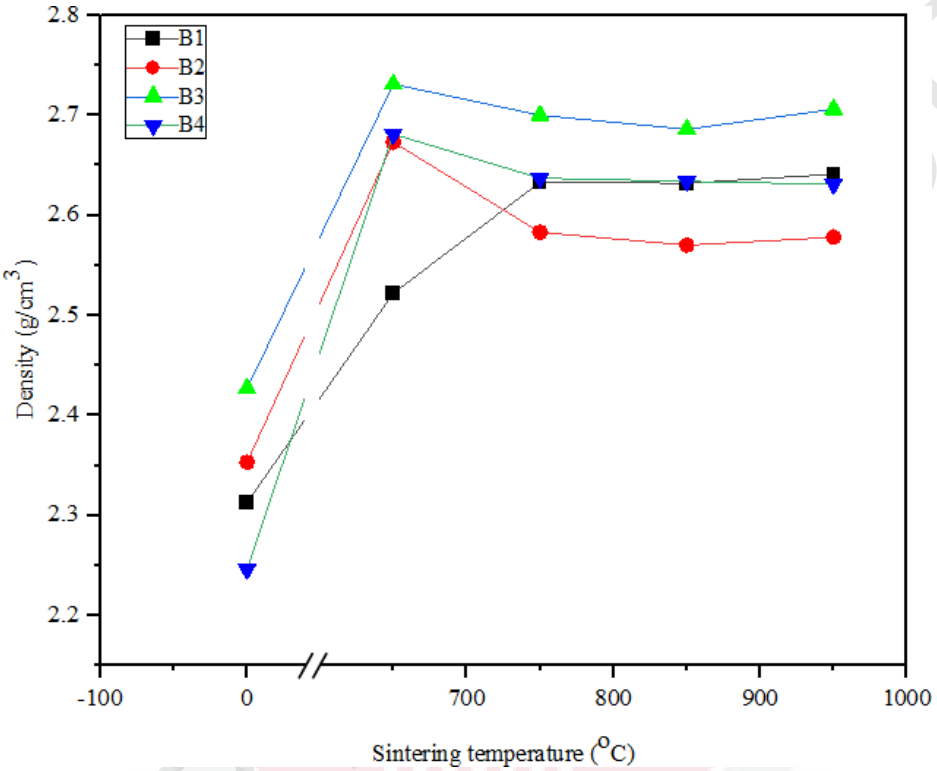

Figure 4.1: Density of different compositions CFAS glass-ceramics at different sintering temperature

Figure 4.1 illustrates the density pattern of CFAS glass-ceramics with different compositions at different sintering temperature. Based on the observation in density data, B3 that containing 7.2 g of CaO and 2.4 g of CaF_2 has the highest density, meanwhile B2 that containing 9.6 g of CaO and not containing CaF_2 has the lowest density after being sintered. At room temperature, 650 °C, 750 °C, 850 °C and 950 °C, the density of B3 is 2.427 g/cm³, 2.731 g/cm³, 2.7 g/cm³, 2.686 g/cm³, and 2.706 g/cm³, respectively.

The patterns of all batches are dramatically increased at temperature of 650 °C, then decreased at temperature of 750 °C except for B1. This is because the heat treatment caused the elimination of moisture in the glass ceramic sample thus increased the kinetic energy in the particles and indirectly increased the density (Gorni G. et al, 2018). The density of B1 is observed to be increased at room temperature to temperature of 750 °C, from 2.552 g/cm³ to 2.633 g/cm³. From the temperature of 750 °C to 950 °C, all batches illustrate small density changes. B2, B3, and B4 show small decrement from 750 °C to 850 °C sinter temperature and all the batches show small increment from 850 °C to 950 °C sintering temperature.

The density increased when the sintering temperature increased but decrease after the temperature reached 1200 °C because the elimination of CO_2 gas throughout the calcite decomposition at high temperature therefore resulted more closed pores in the glass ceramic samples (W.N.W. Jusoh et al, 2019). Based on research, the decrease in density occurred because of the powder agglomeration that occurred during the preparation of the glass ceramics sample (W.N.W. Jusoh et al, 2020).

The type of binders and absorbed moisture were used during the glass ceramic samples preparation caused a weak agglomeration that disturbs the bonds nature therefore affecting the physical properties such as density (Ciftcioglu et al, 1987). Based on Figure 4.1, the density in the sample is increased as it has low CaO and high CaF_2 compositions. This can be clearly observed in Figure 4.1 as B3 has lower CaO and higher CaF_2 compositions compared to B2. Based on research, a glass ceramic sample which has higher CaF_2 composition will have a higher density (W.N.W. Jusoh et al, 2020). This is caused by the CaF_2 that acted as facilitator in the process of crystallization. The viscosity of the glass ceramic samples is lowered by this facilitator by increasing the flow of the broken electrostatic bindings existed in the composition of glass (Mirhadi B. et al, 2012).

4.4 Molar Volume

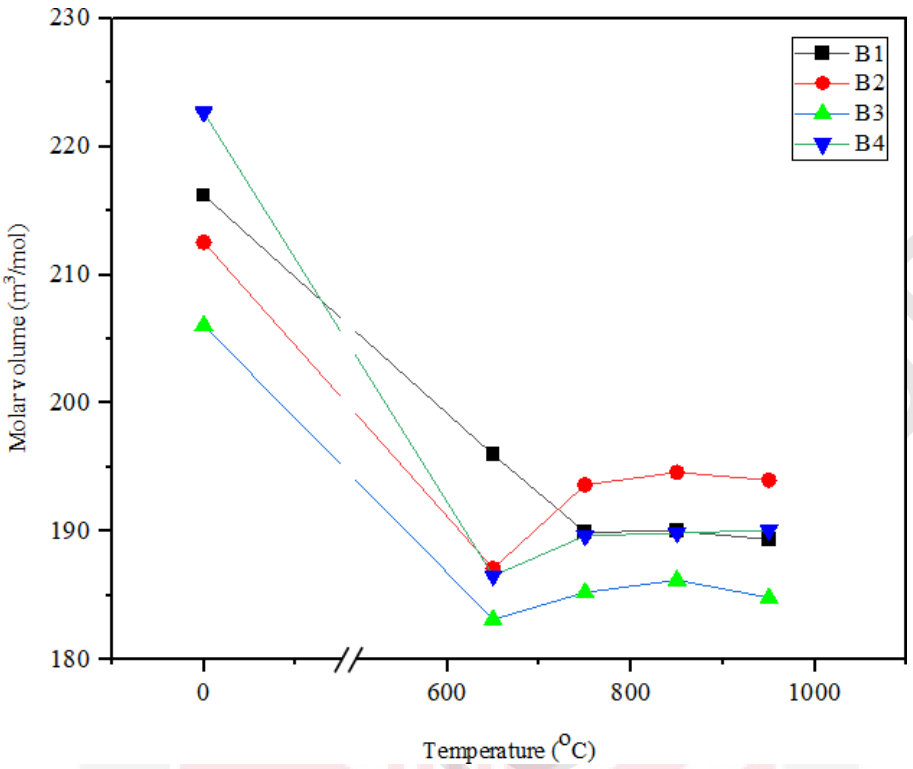

Figure 4.2: Molar volume of different compositions CFAS glass-ceramics at different sintering temperature

Figure 4.2 illustrates the molar volume of different compositions CFAS glass-ceramics at different sintering temperature. At room temperature, B4 has the highest molar volume which is 222.66 m^3/mol then followed by B1, B2, and B3. The lowest molar volume is 206.06 m^3/mol. After the glass ceramic samples were being sintered at 650 °C, the molar volume was dramatically decreased and then showed small changes when the sintering temperature was keep increased to 950 °C. At the sintering temperature of 650 °C, B1 has the highest molar volume which is 195.97 m^3/mol then followed by B2, B4, and B3.

At the sintering temperature of 750 °C, B2 has the highest molar volume which is 193.62 m^3/mol then followed by B1, B4, and B3. At the sintering temperature of 850 °C, B2 has the highest molar volume which is 194.56 m^3/mol then followed by B1, B4, and B3. At the sintering temperature of 950 °C, B2 has the highest molar volume which is 193.99 m^3/mol then followed by B4, B1, and B3. The molar volume decrement is caused by the decrement of interatomic spacing between atoms in the glass ceramic samples (Shahrim M. et al, 2018). The relationship between molar volume and linear shrinkage percentage is inversely related to each other, but different in present glass system (Noorazlan A.M. et al, 2013).

4.5 Linear Shrinkage

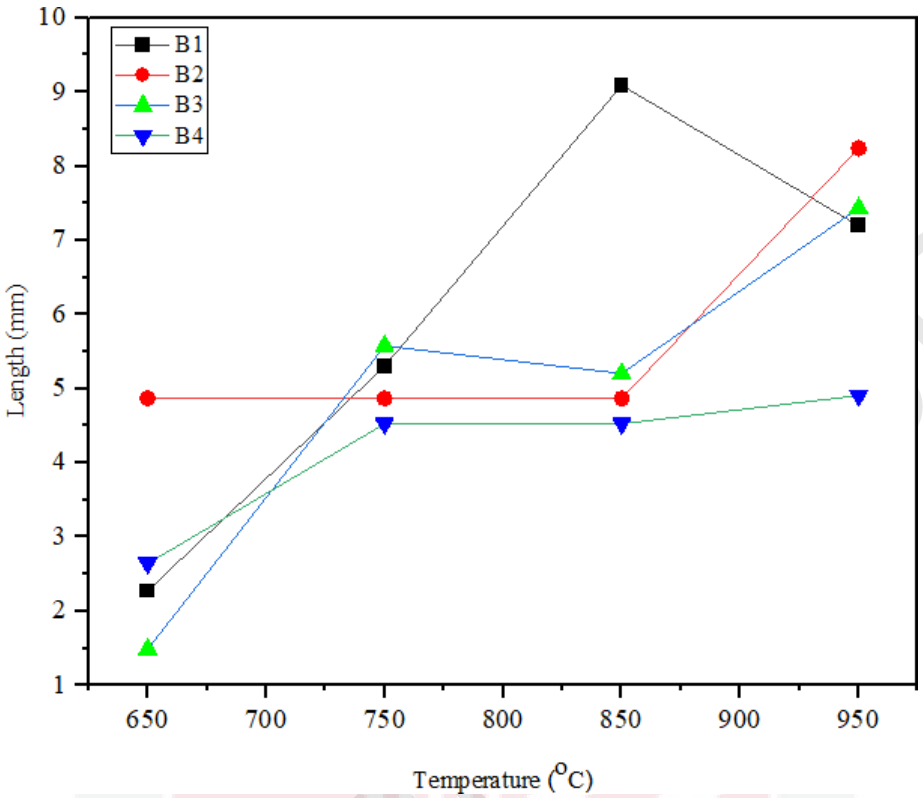

Figure 4.3: Linear shrinkage of different compositions CFAS glass ceramics at different sintering temperature

Figure 4.3 illustrates the linear shrinkage of different compositions CFAS glass ceramics at different sintering temperature. Based on Figure 4.3, B2 recorded the highest linear shrinkage percentage at 650 °C sintering temperature, then followed by B4, B1, and B3. At 750 °C sintering temperature, B3 recorded the highest linear shrinkage percentage, then followed by B1, B2, and B4. For 850 °C sintering temperature, the highest linear shrinkage percentage recorded is B1, then followed by B3, B2, and B4. At 950 °C sintering temperature, it is recorded that B2 is the highest linear shrinkage percentage then followed by B3, B1, and B4.

Overall, the highest linear shrinkage percentage is recorded by B1 at 850 °C sintering temperature which is 9.091% and the lowest shrinkage percentage is recorded by B3 at 650 °C which is 1.487%. When the sample has higher linear shrinkage percentage, it has smaller

volume and size (W.N.W. Jusoh et al, 2019). The rapid increase of linear shrinkage percentage after the samples are sintered at 650 °C and 850 °C is because of the diffusion in the particles that occurred to reduce pores and surface tension (Wah L.C, 2016). As the sintering temperature is increased, the linear shrinkage percentage is increased as well because the temperature increased the materials particles kinetic energy (W.N.W. Jusoh et al, 2019).

This kinetic energy caused the particles in the sample to have high vibration amplitude and induce the diffusion of the particles. Therefore, this resulted the particles to realign themselves into a periodic arrangement (Wah L.C, 2016) (Zaid M.H.M. et al, 2017). The resulting sample will have crystalline and amorphous structure in the reduce of linear shrinkage percentage (W.N.W. Jusoh et al, 2019).

The effect of different CaO and CaF_2 compositions in the CFAS glass ceramic samples of B1, B2, B3, and B4 also played important role in the linear shrinkage percentage. Based on research, linear shrinkage percentage decrease because of the high amount of CaF_2 as it acts as an agent of nucleation where it encourages the formation of crystallization. Therefore, this will increase the size of crystallization as well as the volume and size of sample.

Finally, it will decrease the linear shrinkage percentage of the glass ceramic sample (W.N.W. Jusoh et al, 2020). Meanwhile CaO in the sample reacted to crystallize the glass ceramics and important to contribute to the density and hardness of the sample. As CaO increased, the crystallization activity energy decrease, but if the composition is over the limit, it will cause defects such as lumps, holes, and cracks (Shi P. et al, 2004).

4.6 XRD

Table 4.3: Compositions of Li_2O-Al_2O_3-SiO_2 (LAS) glass-ceramics (wt. %) (Sidek et al., 2017)

Sample	LiO_2	Al_2O_3	SiO_2	MgO	ZnO	CaO	ZrO_2	B_2O_3
LAS1	4	12	64	5.5	5.5	0	4	5
LAS2	4	12	61.9	5.5	5.5	2.1	4	5
LAS3	4	12	59.9	5.5	5.5	4.1	4	5
LAS 4	4	12	57.9	5.5	5.5	6.1	4	5

Table 4.3 shows the GC based on the Li_2O-Al_2O_3-SiO_2 (LAS) were synthesized with different CaO percentage, sintered at 800 °C (Sidek et al., 2017). Figure 4.4 shows the XRD results of the research. All the four samples detected $Li_2OAl_2O_37.5SiO_2$ and ZrO_2 crystal phases but $CaMgSi_2O_6$ phase is only detected in LAS1 which contains no CaO. This indicates that the presence of CaO is important for the $Li_2OAl_2O_37.5SiO_2$ phase formation. As can be seen in Figure 4.4, the increment of CaO compositions in the LAS GC caused the crystal phase of $Li_2OAl_2O_37.5SiO_2$ and ZrO_2 to present in downward trend and the $Li_2OAl_2O_37.5SiO_2$ phase content is slightly increased. Therefore, we expected that the increase of CaO in CFAS may also effect on crystalline phase of CFAS structure.

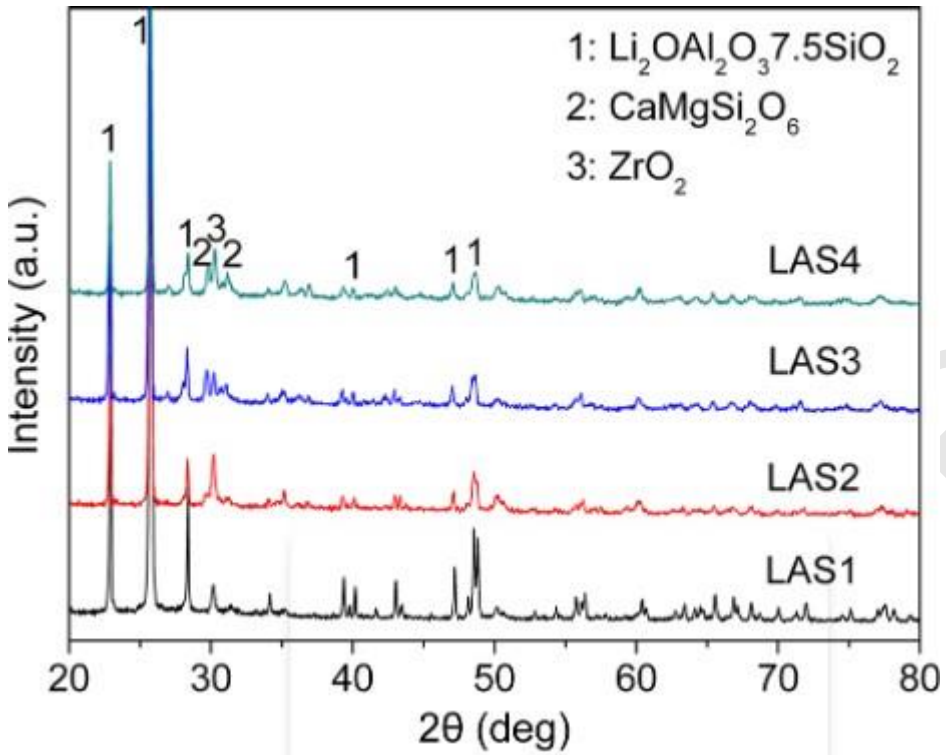

Figure 4.4: XRD data of LAS samples with different CaO percentage sintered at 800 °C (Sidek et al., 2017)

Table 4.4: Samples SiO_2-CaO-Al_2O_3 at different sintering temperatures (Sidek et al., 2017)

Sample (°C)	Sintering Temperature
1	27
2	700
3	800
4	900
5	1000
6	1100

In term of effect sintering temperature, we expect that CFAS will improve the microstructure due the transformation from glass phase crystal phase. This also consistent with the increase density, reduce of molar volume and liner shrinkage of our CFAS sample. In fact, previously study by Almasri et al. (2017) also reported the reduction of glass phase and the increase of phase of triclinic wollastonite (cystal phase) as the sintering temperature increased.

Based on Table 4.4, six wollastonite-based glass-ceramic samples are sintered with different sintering temperatures. Based on this varied sintering temperatures, XRD results are obtained is as shown in Figure 4.5 (Almasri et al., 2017).

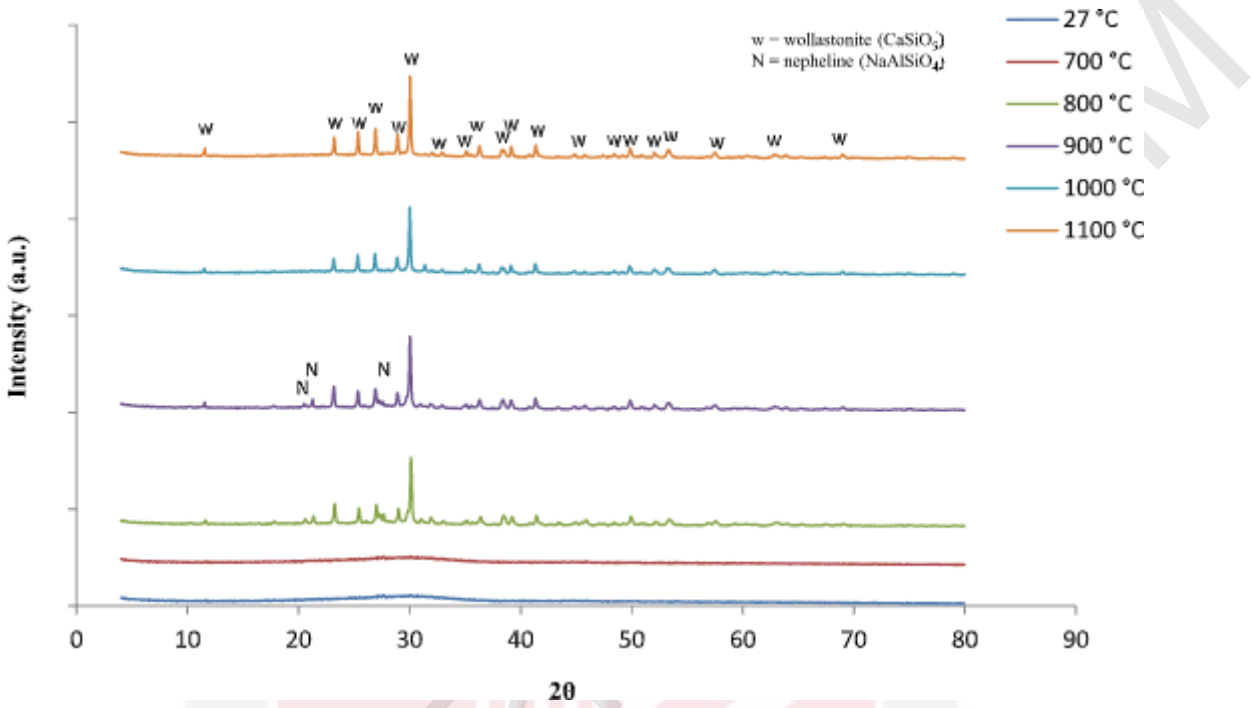

Figure 4.5: XRD results for six different samples of SiO_2-CaO-Al_2O_3 with different sintering temperatures (Almasri et al., 2017)

Figure 4.5 shows the present phases in the precursor glasses. All the sintering process are kept constantly same for all samples, two hours. At room temperature, the XRD result indicated that the GC sample is amorphous as the amorphous hump is detected at 30° of 2θ. At higher temperature, the results indicated the decrement of the glassy phase. At 800°C, the high sintering temperature caused the phase of triclinic wollastonite to nucleate. At 900°C the phase of para wollastonite is nucleated with a little amount of nepheline phase. The nepheline is the minor crystal phase that is detected at diffraction peak of 2θ =21.31°, and 23.18° and 23.18°.

At 1000°C, the intensity of nepheline peak is reduced. This proved that the amount of Al_2O_3 and Na_2O in SLS glass affect the nepheline phase product as be seen in the samples (Almasri et al., 2017).

4.7 SEM

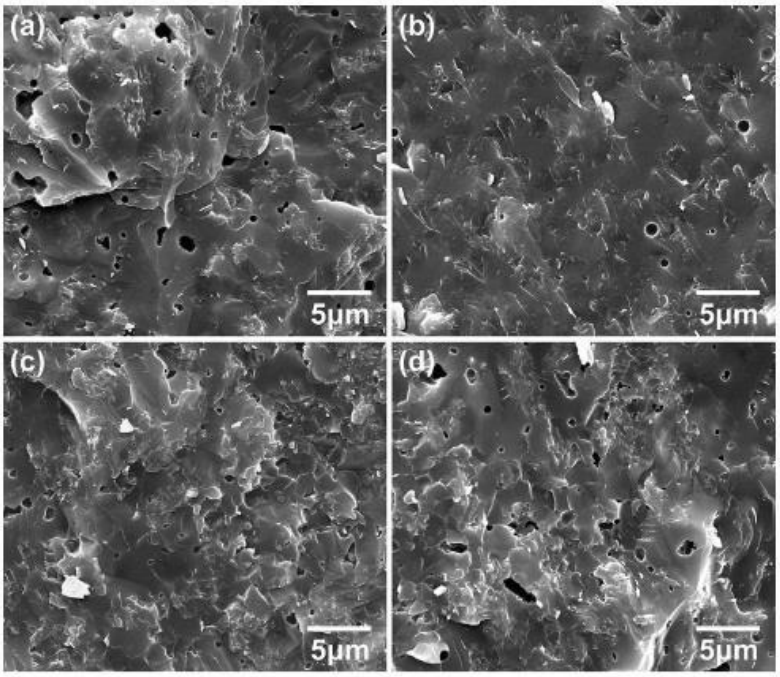

Figure 4.6: SEM images of LAS samples with different CaO percentage sintered at 800 °C (Sidek et al., 2017)

Figure 4.5 shows the SEM images of LAS samples with different CaO percentage sintered at 800 °C. Based on the Figure 4.5, LAS1 (a) which is without CaO, it contains many pores indicating that it has loosen microstructure. However, LAS2 (b) that contained 2.1 wt. % of CaO based on Table 4.1, has the best microstructure among all. As the amount of CaO wt. % increase, the number of pores decreased and exhibits a denser microstructure. But when the CaO is continuously added more than 2.1%, the microstructure begins to deteriorate (Sidek et al., 2017). This also consistent with our result of density, reduce of molar volume and linear shrinkage. Therefore, we expect that the overall morphology of CFAS may having reduction of pores as the CaO is increased.

CHAPTER 5

CONCLUSION

5.1 Conclusion

The conclusions that can be made in this study is calcium fluoroaluminosilicate (CFAS) bioglass-ceramic can be synthesized by varying its calcium oxide (CaO) percentage compositions at different sintering temperatures. The GC samples are synthesized by using the melt quenching method technique. The study of structure of the GC samples are characterized by density, linear shrinkage percentage, molar volume and XRD.

Subsequently, the samples undergo sintering process. Based on XRF results, the compositions can be determined. The density increased when the sintering temperature increased but decrease after the temperature reached 1200 °C. The molar volume decrement is caused by the decrement of interatomic spacing between atoms in the glass ceramic samples.

The relationship between molar volume and linear shrinkage percentage is inversely related to each other, but different in present glass system. Based on the linear shrinkage results, as the sintering temperature is increased, the linear shrinkage percentage is increased as well because the temperature increased the materials particles kinetic energy. Based on research, linear shrinkage percentage decrease because of the high amount of CaF_2 as it acts as an agent of nucleation where it encourages the formation of crystallization. Therefore, this will increase the size of crystallization as well as the volume and size of sample.

5.2 Future Works

- Characterize by using Thermogravimetric Analysis (TGA) to measure the variations in the mass of GC samples while the temperature is altered in a controlled way.
- Characterize by using Scanning in Differential Mode Calorimetry (DSC) to monitor the variations in heat flow to and from the samples when the temperature is altered.
- Characterize by using Field Emission Scanning Electron Microscopy (FESEM) to study the elemental information and topography of the GC samples.
- Characterize by using Fourier Transform Infrared Spectroscopy (FTIR) that uses infrared light to observe the chemical properties and scan test the GC samples.

REFERENCE

A. A. S. Staff, "What is XRF (X-ray Fluorescence) and How Does it Work?," *ThermoFisher Scientific*, 2020. https://www.thermofisher.com/blog/ask-a-scientist/what-is-xrf-x-ray-fluorescence-and-how-does-it-work/.

A. H. Simon, S. M. Hues, and L. Lovejoy, "X-Ray Fluorescence Spectroscopy Ultratrace Impurity Analysis of Wafer Surfaces Physicochemical characterization of nanomaterials : polymorph , composi- Absorption of Nuclear Radiation Bioinorganic Fundamentals and Appli- cations : Metals in Natural Living," 2020.

A. Imtiaz, M. A. Farrukh, M. Khaleeq-ur-rahman, and R. Adnan, "Micelle-Assisted Synthesis of Al2O3 · CaO Nanocatalyst : Optical Properties and Micelle-Assisted Synthesis of Al 2 O 3 · CaO Nanocatalyst : Optical Properties and Their Applications in Photodegradation of 2 , 4 , 6-Trinitrophenol," no. November, 2013, doi: 10.1155/2013/641420.

A. J. Salinas, "Silica-based Ceramics : Glasses," no. Iv, 2014.

A. Stamboulis, R. G. Hill, and R. V. Law, "Characterization of the structure of calcium alumino-silicate and calcium fluoro-alumino-silicate glasses by magic angle spinning nuclear magnetic resonance (MAS-NMR)," *J. Non. Cryst. Solids*, vol. 333, no. 1, pp. 101–107, 2004.

Baino F, Novajra G, Miguez-Pacheco V, Boccaccini AR, Vitale- Brovarone C. Bioactive glasses: Special applications outside the skeletal system. J Non- Cryst Solids 2016;432:15–30.

B. Karmakar, Functional Glasses and Glass-Ceramics: Processing, Properties and Applications. Butterworth-Heinemann, 2017.

Brinker, C. J.; G. W. Scherer (1990). Sol-Gel Science: The Physics and Chemistry of Sol-Gel Processing. Academic Press. ISBN 978-0-12-134970-7.

Britannica, T. Editors of Encyclopaedia (2021, May 6). Glass. Encyclopedia Britannica. https://www.britannica.com/technology/glass

B. J. A. Moulton, G. S. Henderson, I. Farooq, R. G. Hill, and D. Biomaterials, "Glasses : Alkali and Alkaline-Earth Sili- cates Bioactive glasses — structure and appli- cations Reverse Monte Carlo Methods for Structural Modelling," 2021.

Brauer, D. S., Anjum, M. N., Mneimne, M., Wilson, R. M., Doweidar, H., & Hill, R. G. (2012). Fluoride-containing bioactive glass-ceramics. *Journal of Non- Crystalline Solids*, *358*(12–13), 1438–1442.

Ciftcioglu, M., Akinc, M., & Burkhart, L. (1987). Effect of agglomerate strength on sintered density for yttria powders containing agglomerates of monosize spheres. *Journal of the American Ceramic Society*, *70*(11), C-329.

C. T. Ridgely, "Archimedes' principle in general coordinates," *Eur. J. Phys.*, vol. 31, no. 3, pp. 491–499, May 2010.

D. A. Chareev, "Experimental Aspects of Plat- inum-Group Minerals Densification Mechanisms of Oxide Glasses and Melts," 2019.

Doremus, R.H. Glass Science; Wiley: New York, NY, USA, 1994.

D. S. Brauer, M. N. Anjum, M. Mneimne, R. M. Wilson, H. Doweidar, and R. G. Hill, "Fluoride-containing bioactive glass-ceramics," *J. Non. Cryst. Solids*, vol. 358, no. 12–13, pp. 1438–1442, 2012.

E.S. Kim, W.J. Yeo, Thermal properties of CaMgSi2O6 glass– ceramics with Al2O3. Ceram. Int. 38(Suppl 1), S547–S550 (2012)

El-Ghannam, A., & Ducheyne, P. (2011). Bioactive ceramics. In *Comprehensive Biomaterials* (Vol. 1, pp. 157–179). Elsevier.

E. Van Der Linden, E. A. Foegeding, and B. Science, "Gelation Gelation How Lipid Cores Affect Lipid Nanopar- ticles as Drug and Gene Delivery Sys- tems Silk hydrogels for tissue engineering and dual-drug delivery," 2021.

Furnaces: principles of design and use. (1982). In *The Efficient Use of Energy* (pp. 116–165). Elsevier.

Gutzow, I.S.; Schmelzer, J.W.P. The Vitreous State—Thermodynamics, Structure, Rheology, and Crystallization, 2nd ed.; Springer: Berlin, Germany, 2013; ISBN 978-3-642-34633-0.

G.H. Chen, X.Y. Liu, Fabrication, characterization and sintering of glass-ceramics for low-temperature co-fired ceramic substrates. J. Mater. Sci. Mater. Electron. 15(9), 595–600 (2004)

G. Valverde Aguilar, "Introductory Chapter: A Brief Semblance of the Sol-Gel Method in Research," in *Sol-Gel Method - Design and Synthesis of New Materials with Interesting Physical, Chemical and Biological Properties*, 2019.

Gorni G., Pascual M.J., Caballero A., Velázquez J.J., Mosa J., Castro Y., Durán A. (2018): Crystallization mechanism in sol-gel oxyfluoride glass-ceramics. Journal of Non Crystalline Solids, 501, 145-152.

Hench LL (Ed.), An Introduction to Bioceramics, 2nd ed., London, UK: Imperial College Press; 2013.

Hench LL. The future of bioactive ceramics. J Mater Sci: Mater Med 2015;26:1–4.

Hench, L. L.; J. K. West (1990). "The Sol-Gel Process". Chemical Reviews. 90: 33–72.

Holand W, Beall G. Glass-Ceramic Technology, 2nd ed., USA: The American Ceramic Society & Wiley; 2012.

Hoppe, A., & Boccaccini, A. R. (2014). Bioactive glass foams for tissue engineering applications. In *Biomedical Foams for Tissue Engineering Applications* (pp. 191–212). Elsevier Ltd.

H. Pirayesh and J. A. Nychka, "Sol-gel synthesis of bioactive glass-ceramic 45S5 and its in vitro dissolution and mineralization behavior," *J. Am. Ceram. Soc.*, vol. 96, no. 5, pp. 1643–1650, 2013.

I. Ions, S. Dioxide, B. D. Boyan, S. M. Carvalho, and P. Ducheyne, "Biomaterials and Clinical Use Bioactive Glass Nanoparticles for Periodontal Regeneration and Applications in Dentistry Metallic , Ceramic , and Polymeric Bio- materials Volume 1 Biomaterials in treatment of orthope- dic infections Bioactive glasses and ," 2017.

Jusoh, W. N. W., Matori, K. A., Zaid, M. H. M., Zainuddin, N., Khiri, M. Z. A., Rahman, N. A. A., Jalil, R. A., & Kul, E. (2019). Effect of sintering temperature on physical and structural properties of Alumino-Silicate-Fluoride glass ceramics fabricated from clam shell and sodalime silicate glass. *Results in Physics*, *12*, 1909–1914.

Jusoh, W. N. W., Matori, K. A., Zaid, M. H. M., Zainuddin, N., Khiri, M. Z. A., Rahman, N. A. A., Jalil, R. A., & Kul, E. (2020). Influence of different CaF2 contents and heat treatment temperatures on apatite-mullite glass ceramics derived from waste materials. *Ceramics - Silikaty*, *64*(4), 447–459.

J. M. F. Ferreira, "Bioactive Glasses and Glass-Ceramics for Healthcare Applications in Bone Regeneration and Tissue Engineering," pp. 1–54, 2018.

Jones, J.; Clare, A.G. (Eds.) Bio-Glasses: An Introduction; John Wiley and Sons, Ltd.: Chichester, UK, 2012; ISBN 9780470711613.

Kokubo T, Bioceramics and their clinical applications, USA: Woodhead publishing limited; 2008.

Kokubo T. Bioactive glass-ceramics: Properties and applications. Biomaterials 1991;12:155–163.

Klein, L. (1994). Sol-Gel Optics: Processing and Applications. Springer Verlag. ISBN 978-0-7923-9424-2.

K. T. Hench L.L., *Properties of bioactive glasses and glass-ceramics*. Springer, Boston, MA, 1998.

Li, B., Qing, Z., Li, Y., Li, H., & Zhang, S. (2016). Effect of CaO content on structure and properties of low temperature co-fired glass–ceramic in the Li2O–Al2O3–SiO2 system. *Journal of Materials Science: Materials in Electronics*, *27*(3), 2455–2459. https://doi.org/10.1007/s10854-015-404

M. Montazerian and E. D. Zanotto, "Review Article History and trends of bioactive glass-ceramics," pp. 1231–1249, 2016, doi: 10.1002/jbm.a.35639.

Mirhadi B., Mehdikhani B. (2012): Effect of calcium fluoride on sintering behavior of SiO2–CaO–Na2O–MgO glass-ceramic system. Processing and Application of Ceramics, 6, 159-164. doi: 10.2298/PAC1203159M

Miguez-Pacheco V, Hench LL, Boccaccini AR. Bioactive glasses beyond bone and teeth: Emerging applications in contact with soft tissues. Acta Biomater 2015;13:1–15.

Montazerian M, Singh SP, Zanotto ED. An analysis of glass- ceramic research and commercialization. Am Ceram Soc Bull 2015;94:30–35.

Mauro, J.C.; Loucks, R.J.; Varshneya, A.K.; Gupta, P.K. Enthalpy landscapes and the glass transition. Sci. Model. Simul. 2008, 15, 241–281.

Mohadi, R., Anggraini, K., Riyanti, F., & Lesbani, A. (2016). *Preparation Calcium Oxide (CaO) from Chicken Eggshells*. *August*. https://doi.org/10.22135/sje.2016.1.2.32-35

M. Methods, "processes A Comparison of Bioactive Glass Sca ff olds Fabricated by Robocasting from Powders Made by Sol – Gel and," 2020.

M. T. Hincke, Y. Nys, J. Gautron, K. Mann, A. B. Rodriguez-Navarro, and M. D. McKee, "The eggshell: Structure, composition and mineralization," *Front. Biosci.*, vol. 17, no.

4, pp. 1266–1280, 2012, doi: 10.2741/3985.

M. Z. A. Khiri *et al.*, "Soda lime silicate glass and clam Shell act as precursor in synthesize calcium fluoroaluminosilicate glass to fabricate glass ionomer cement with different ageing time," *J. Mater. Res. Technol.*, vol. 9, no. 3, pp. 6125–6134, 2020, doi: 10.1016/j.jmrt.2020.04.015.

M. Z. A. Khiri *et al.*, "Soda lime silicate glass and clam Shell act as precursor in synthesize calcium fluoroaluminosilicate glass to fabricate glass ionomer cement with different ageing time," *J. Mater. Res. Technol.*, vol. 9, no. 3, pp. 6125–6134, 2020, doi: 10.1016/j.jmrt.2020.04.015.

Montazerian, M., & Zanotto, E. D. (2016). *Review Article History and trends of bioactive glass-ceramics*. 1231–1249. https://doi.org/10.1002/jbm.a.35639

Nazopatul, P. H., Irmansyah, & Irzaman. (2018). Extraction and characterization of silicon dioxide from rice straw. *IOP Conference Series: Earth and Environmental Science*, *209*(1). https://doi.org/10.1088/1755-1315/209/1/012013

Noorazlan, A. M., Kamari, H. M., Zulkefly, S. S., & Mohamad, D. W. (2013). Effect of erbium nanoparticles on optical properties of zinc borotellurite glass system. Journal of Nanomaterials, 2013, 168.

N. Nezafati, F. Moztarzadeh, S. Hesaraki, and M. Mozafari, "Synergistically reinforcement of a self-setting calcium phosphate cement with bioactive glass fibers," vol. 37, pp. 927–934, 2011, doi: 10.1016/j.ceramint.2010.11.002.

N. P., K. Srinivasan, A. Adhikari, and L. Satapathy, "Evaluation of Calcium Fluoroaluminosilicate Based Glass Ionomer Luting Cements Processed Both by Conventional and Microwave Assisted Methods," *Technologies*, vol. 3, no. 2, pp. 58–73, Mar. 2015, doi: 10.3390/technologies3020058.

P. Pentoxide, "Phosphorus Pentoxide Spotlight 138," pp. 2545–2546, 2002, doi: 10.1055/s-2005-917086.

Paul, A. Chemistry of Glasses, 2nd ed.; Chapman and Hall: Boca Raton, FL, USA, 1990.

R. M. Albadr and K. Ziadan, "Preparation and characterization of Calcium-Fluoroaluminosilicate glass fillers for dental composite ," *Basrah J. Sci.*, no. January, 2015.

Salinas AJ, Vallet-Regı M. Bioactive ceramics: From bone grafts to tissue engineering. RSC Adv 2013;3:11116–11131.

Shelby, J. Introduction to Glass Science and Technology, 2nd ed.; The Royal Society of Chemistry: Cambridge, UK, 2005; ISBN 0854046399.

Shi, P. & Jiang, M. & Liu, C. & Wang, D. & Zhu, M.. (2004). Effect of CaO on glass ceramics crystallization and properties of CaO-A12O3-SiO2 system. 32. 1389-1393.

Shahrim Mustafa, I., Abdul Rahman, A., Ishak, H., & Aida Abdul Azim, N. (2018). Effect of Sintering Temperature on Silica Based Glass-Ceramics Derived From Soda-Lime-Silica Glass. In *J .Sol. State Sci. & Technol. Letts* (Vol. 19, Issue 2).

Salinas AJ, Vallet-Regı M. Bioactive ceramics: From bone grafts to tissue engineering. RSC Adv 2013;3:11116–11131.

Tangboriboon, N., Kunanuruksapong, R., Sirivat, A., Kunanuruksapong, R., & Sirivat, A. (2012). Preparation and properties of calcium oxide from eggshells via calcination. *Materials Science- Poland*, *30*(4), 313–322. https://doi.org/10.2478/s13536-012-0055-7

Tangboriboon, N., Kunanuruksapong, R., Sirivat, A., Kunanuruksapong, R., & Sirivat, A. (2012). Preparation and properties of calcium oxide from eggshells via calcination. *Materials Science- Poland*, *30*(4), 313–322. https://doi.org/10.2478/s13536-012-0055-7

T. Kokubo, "Bioactive glass ceramics: properties and applications," *Biomaterials*, vol. 12, no. 2, pp. 155–163, Mar. 1991, doi: 10.1016/0142-9612(91)90194-F

Vallet-Regi, M. (Ed.) Bioceramics with Clinical Applications; John Wiley & Sons Ltd.: Chichester, UK, 2014.

V. A. Solé, E. Papillon, M. Cotte, P. Walter, and J. Susini, "A multiplatform code for the analysis of energy-dispersive X-ray fluorescence spectra," *Spectrochim. Acta - Part B At. Spectrosc.*, vol. 62, no. 1, pp. 63–68, Jan. 2007, doi: 10.1016/j.sab.2006.12.002.

Wah LC. Effects of heat treatment on structure and thermal diffusivities of SiO2-Na2O-Al2O3-CaO-CaF2 glass-ceramics from waste materials (master's thesis).Malaysia: Universiti Putra Malaysia; 2016.

W. Höland, G. H. Beall, Glass Ceramic Technology. John Wiley & Sons, 2012.

"X-Ray diffraction (XRD)," *Anton Paar*, 2021. https://wiki.anton-paar.com/en/x-ray-diffraction-xrd/.

Zaid MHM, Matori KA, Sidek AA, Wahab ZA, Rashid SSA. Effect of sintering on crystallization and structural properties of soda lime silica glass. Sci Sintering 2017;49:409–17.

Zanotto ED. A bright future for glass–ceramics. Am Ceram Soc Bul 2010;89:19–27.

Zhou Y.L., Huan Z.G., Chang J. (2015) *Silicate-Based Bioactive Composites for Tissue Regeneration.* In: Antoniac I. (eds) Handbook of Bioceramics and Biocomposites. Springer, Cham. https://doi.org/10.1007/978-3-319-09230-0_15-1

Z. Khurshid, A. S. Khan, and C. Appli-, "Learn more about melt quenching Novel Techniques of Scaffold Fabrica- tion for Bioactive Glasses Silver-containing bioactive glasses for tissue engineering applications," 2019.

Z. Khurshid, A. S. Khan, and C. Appli-, "Novel Techniques of Scaffold Fabrica- tion for Bioactive Glasses Silver-containing bioactive glasses for tissue engineering applications," 2020.

APPENDICES

Operator : noriza

Comment : Oxide, Air, 2chan

Group : easy-Air-Oxide

Date : 2021-11-15 11:30:22

Measurement Condition

Instrument : EDX-720 Atmosphere : Air Collimator : 10(mm) Spin : No

---

Analyte	TG	kV	uA	FI	Acq.(keV)	Anal.(keV)	Time(sec)	DT(%)
Ti-U	Rh	50	59	Auto	---- 0 - 40	0.0 - 40.0	Live - 100	40
Na-Sc	Rh	15	275	Auto	---- 0 - 20	0.0 - 4.4	Live - 100	40

Peak List

Channel	Line	keV	Net Int.(cps/uA)
Ti-U	CaKaESC	1.94	1.8016
	CaKbESC	2.26	0.2780
	RhLa	2.68	0.9180
	----	2.92	1.7941
	K Ka	3.24	1.8354
	K Kb	3.58	0.2570
	CaKa	3.68	221.3644
	CaKb	4.02	34.6328
	ErLa	7.04	0.2297
	CaKaSUM	7.40	1.1380
	Ca SUM	7.72	0.4415
	CuKa	8.02	0.2418
	SrKa	14.18	2.1231

	SrKb	15.86	0.3984
	ZrKa	15.86	0.1304
	RhKaC	19.12	5.5279
	RhKa	20.22	9.5185
	RhKbC	21.36	1.0634
	----	21.88	0.6003
	RhKb	22.78	1.6562

Na-Sc	CaKaESC	1.95	0.5620
	CaKbESC	2.29	0.0867
	RhLa	2.70	0.2625
	PdLa	2.85	0.3792
	PdLg1	3.31	0.0095
	K Ka	3.31	0.1898
	K Kb	3.59	0.0265
	CaKa	3.70	63.7244
	CaKb	4.03	9.1631
	ScKa	4.09	0.0348
	ScKb	4.49	0.0390
	----	5.32	0.0422
	CaKaSUM	7.40	0.4342
	Ca SUM	7.72	0.1209

Quantitative Result

Analyte	Result	Std.Dev.	Proc.-Calc.	Line	Int.(cps/uA)

CaO	99.480 %	(0.076)	Quan-FP	CaKa	63.7244
K2O	0.258 %	(0.011)	Quan-FP	K Ka	0.1898
Sc2O3	0.107 %	(0.056)	Quan-FP	ScKa	0.0348
Er2O3	0.068 %	(0.004)	Quan-FP	ErLa	0.2297

SrO	0.061 %	(0.001)	Quan-FP	SrKa 2.1231
CuO	0.022 %	(0.001)	Quan-FP	CuKa 0.2418
ZrO2	0.004 %	(0.001)	Quan-FP	ZrKa 0.1304

Sample : SLS

Operator : noriza

Comment : Oxide, Air, 2chan

Group : easy-Air-Oxide

Date : 2021-11-15 11:37:44

Measurement Condition

Instrument : EDX-720 Atmosphere : Air Collimator : 10(mm) Spin : No

---

Analyte	TG	kV	uA	FI	Acq.(keV)	Anal.(keV)	Time(sec)	DT(%)
Ti-U	Rh	50	89-Auto	----	0 - 40	0.0 - 40.0	Live - 100	40
Na-Sc	Rh	15	1000-Auto	----	0 - 20	0.0 - 4.4	Live - 100	35

Peak List

Channel	Line	keV	Net Int.(cps/uA)
Ti-U	SiKa	1.72	0.6429
	RhLa	2.68	0.4372
	AcMa	2.94	0.3888
	AgLa	2.94	0.1455
	K Ka	3.30	0.2663
	K Kb	3.58	0.0373
	CaKa	3.70	19.1932
	CaKb	4.02	3.1774
	ScKa	4.08	1.9485
	ScKb	4.50	0.2728
	CrKa	5.40	0.1424
	FeKa	6.40	2.5155
	CoKa	6.94	0.8986

	NiKa	7.46	0.1621
	CoKb	7.64	0.1220
	CuKa	8.04	0.2800
	ZnKa	8.66	2.4641
	ZnKb	9.58	0.4085
	----	10.56	0.5081
	AcLa	12.66	0.3509
	SrKa	14.16	1.1331
	AcLb1	15.72	0.1687
	ZrKa	15.78	5.2100
	SrKb	15.84	0.3134
	ZrKb	17.68	0.9422
	RhKaC	19.20	10.0427
	RhKa	20.24	8.4841
	RhKbC	21.42	1.7445
	----	22.10	0.4255
	RhKb	22.78	1.2988

Na-Sc	SiKa	1.75	0.3324
	CaKaESC	1.96	0.0541
	S Ka	2.31	0.0230
	RhLa	2.71	0.2484
	----	2.98	0.2099
	K Ka	3.34	0.0469
	K Kb	3.59	0.0066
	CaKa	3.71	6.6252
	CaKb	4.03	1.0108
	ScKa	4.09	0.0839
	ScKb	4.52	0.0894
	CrKa	5.42	0.0358
	FeKa	6.42	0.4383
	CoKa	6.94	0.1087

FeKb	7.06	0.0658
ZnKa	8.64	0.1958
ZnKb	9.62	0.0431

Quantitative Result

Analyte	Result	Std.Dev.	Proc.-Calc.	Line	Int.(cps/uA)
SiO2	59.504 %	(0.349)	Quan-FP	SiKa	0.3324
CaO	36.644 %	(0.046)	Quan-FP	CaKa	6.6252
Fe2O3	1.031 %	(0.008)	Quan-FP	FeKa	2.5155
SO3	0.771 %	(0.037)	Quan-FP	S Ka	0.0230
Sc2O3	0.490 %	(0.020)	Quan-FP	ScKa	0.0839
ZnO	0.359 %	(0.003)	Quan-FP	ZnKa	2.4641
K2O	0.330 %	(0.012)	Quan-FP	K Ka	0.0469
Co2O3	0.291 %	(0.005)	Quan-FP	CoKa	0.8986
ZrO2	0.281 %	(0.002)	Quan-FP	ZrKa	5.2100
Cr2O3	0.110 %	(0.007)	Quan-FP	CrKa	0.1424
SrO	0.063 %	(0.001)	Quan-FP	SrKa	1.1331
CuO	0.049 %	(0.002)	Quan-FP	CuKa	0.2800
Ac	0.039 %	(0.002)	Quan-FP	AcLa	0.3509
NiO	0.038 %	(0.003)	Quan-FP	NiKa	0.1621

PERSONAL INFO

Date of Birth : 7th of May 1999
Nationality : Malaysian
Ethnicity : Malaysian

CONTACT ME AT

Address:
Batu Pahat, Johor.

e-mail:
mimiadilah04@gmail.com

Phone number:
+6017-7176231
+607 4186158

LinkedIn account:
https://www.linkedin.com/in/mimi-adilah-b11178199

SKILLS SUMMARY

- Project Management
- Teamwork
- Volunterism
- Lab Handling
- Communication Skills
- Multitasking

POSITIONS

- QA Trainee at Top Glove Berhad
- Publicity Committee Member during Kursus Kepimpinan Mahasiswa Kolej Tun Dr. Ismail (KUKEM) (2019), Physics Fusion Day (2018,2019,2020), Science Ace Carnival UPM (2021).
- Activity Committee Member during Physics Outreach program and Karnival Jom Sains (KJS) (2019-2020)

MIMI NUR `ADILAH BINTI SAMAD

BACHELOR OF SCIENCE IN MATERIALS SCIENCE WITH HONOURS

PERSONAL PROFILE

I am a bachelor of science undergraduate student from Universiti Putra Malaysia with holistic knowledge of materials science and internship experience from Top Glove Corporation Berhad. I am eager to learn more and ready to work at your esteemed company.

EXPERIENCES

Student Representative Council
Kolej Tun Dr. Ismail | March 2020 - July 2021

- Conduct day-to-day project coordination, planning, and implementation across multiple teams
- Cooperative in teamwork to manage programs.
- Dedicated to manage college events involving college students throughout the year.

Active in Volunteerism
Kelab Huffaz | YoSH | Jan 2018 - present

- Managed complex projects as from start to finish
- Collaborated with other students from different universities such as Al-Azhar University, Universiti Teknologi PETRONAS, Universiti Teknologi Nasional and few more.
- Committed to work at many places such as Rumah Seri Kenangan nursing home at Melaka, Pusat Hafazan An-Nur at Pahang, Sekolah Kebangsaan Labu Besar at Perak, Seremban Girls' School at Negeri Sembilan.

EDUCATIONAL HISTORY

Universiti Putra Malaysia
Bachelor of Science in Materials Science with Honours | March 2018 - July 2022

- Current GPA 3.750 and CGPA 3.367

Universiti Putra Malaysia
Foundation of Agricultural Science | June 2017 - May 2018

- CGPA 3.419

Sekolah Menengah Kebangsaan Dato' Sulaiman
Sijil Pelajaran Malaysia (SPM) | 2012 - 2016

- 3A+ 2A 2A- 2B+

RELEVANT COURSES

- Solid State Physics
- Modern Physics
- Magnetism and Magnetic Materials
- Thermodynamics
- Electromagnetism
- Electronics
- Ceramics and Polymer
- Metal and Alloys
- Geometrical and Wave Optics
- Semiconductor Devices
- Semiconductor Technology
- Materials Processing Technology
- Superconductor
- Semiconductor Devices
- Semiconductor Technology
- Advanced Materials
- Quality Management System in Science
- Innovation for Scientist
- Computer Programming 1
- Analytical Method of Structure and Microstructure

SCAN ME

SOFTWARE SKILLS

Microsoft Office

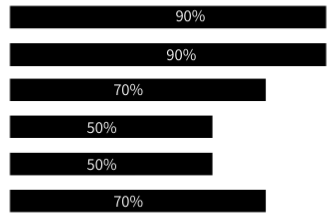

WORKING EXPERIENCES

Top Glove Corporation Berhad

Klang | 2022

Trainee, Quality Assurance (QA)

- Conducted analysis on in process compliance as instructed by Supervisor
- Completed project related to Quality Assurance to improve process efficiency and eliminating process wastages
- Took ad hoc task that was assigned by Supervisor

Projects

1. QA IPQC Prediction Model of Glove Weight Defect

- Assisted in generating MATLAB apps by using the collected process parameters data from Power BI and laboratory tests

2. QA IPQC PowerApps Analysis

- Analyzed data from Microsoft PowerApps portal for bug fixing

3. QA IPQC Dirt Campaign Analysis

- Made analysis from data in Microsoft Teams to identify issues for QA enforcements

REFERENCES

Reference 1: Academic Advisor

Dr Shuhazlly Mamat @Mat Nazir
Senior Lecturer (Dr.)
Department of Physics Universiti Putra Malaysia
Tel: 03 89468872
Fax: 03-89454454
e-mail: shuhazlly@upm.edu.my

Reference 2: Industrial Supervisor

Mr. Saiyidinzam b. Abdul Hamid
Executive II, Quality Assurance
Top Glove Corporation Berhad
F30, Lot 4969, Jalan Teratai, Batu 6, Off Jalan Meru,
41050 Klang, Selangor Darul Ehsan.
Tel: +6012-6488487
e-mail: saiyidinizam@topglove.com.my